# Multi-Component LFM Signal Parameter Estimation for Symbiotic Chirp-UWB Radio Systems

Zhaoxi Wen, Mingqian Liu, *Member, IEEE*, Yunfei Chen, *Senior Member, IEEE*, Nan Zhao, *Senior Member, IEEE*, Arumugam Nallanathan, *Fellow, IEEE* and Xiaoniu Yang

***Abstract*—Symbiotic chirp-ultra wide bandwidth (UWB) radio system (SCURS) is a UWB radio system with the symbiosis of linear frequency modulation (LFM) and orthogonal frequency division multiplexing (OFDM) signals. It has a high data rate and can transmit data on two channels simultaneously. Moreover, multi-component LFM (MCLFM) parameter estimation plays an important role in the demodulation of SCURS. Furthermore, the complex electromagnetic environment also brings impulsive noise. In this paper, a novel parameter estimation method for MCLFM signals based on the fractional Fourier transform-bald eagle search algorithm (FRFT-BES) and synchroextracting short-time fractional Fourier transform-Hough (SSFT-Hough) with alpha-stable noise is proposed. First, we use a nonlinear transformation to eliminate the negative effect of alpha-stable noise on parameter estimation. Second, we combine the improved BES with FRFT to propose FRFT-BES and use it to estimate the frequency modulation rate. Finally, we propose a new time-frequency (TF) transform method with high TF resolution as SSFT, and we combine it with Hough transform (HT) to propose SSFT-Hough to estimate the initial frequency. Frequency modulation rate and initial frequency are widely used in MCLFM signals separation. Simulation results demonstrate that the proposed method performs well in low mixed signal-to-noise ratio (MSNR), and it is superior to existing methods.**

***Index Terms*—Alpha-stable noise, multi-component signals, parameter estimation, symbiotic communication.**

## I. Introduction

LINEAR frequency modulation (LFM) signal is a kind of large time-bandwidth product signal [1]. It has many advantages, such as high range resolution, low intercept probability, excellent radial velocity resolution, and large Doppler tolerance [2]. Thus, it plays an important role in wireless applications, and because wireless applications are widely used [3], such as cognitive radios [4], LFM signals have been thoroughly studied in radar, communication, sonar, target tracking, and other fields [5]. In recent years, due to the significant increase in the quantity and type of signals in the electromagnetic environment and the interaction of various electrical devices, the electromagnetic environment has become more and more complex [6], [7]. Meanwhile, with the rapid development of Internet of Things (IoT), radio frequency (RF) signals are widely studied and used in communications [8], [9], such as backscatter communications [10]–[14], and the concept of symbiosis has gradually been applied to various fields [15]. The symbiotic chirp-ultra wide band (UWB) radio system (SCURS) is a novel UWB radio system. It combines the multi-component LFM (MCLFM) with specially designed orthogonal frequency division multiplexing (OFDM) signals in RF combiner. SCURS has many advantages, for example, it can simultaneously transmit two channels of data at high rate. When demodulation is performed at the receiving end of SCURS, MCLFM parameter estimation needs to be implemented for demodulation. The most important parameters for demodulation are frequency modulation rate and initial frequency. In a complex electromagnetic environment with impulsive characteristics, due to a variety of natural and human factors, such as lightnings, tsunamis, and the switching of switches, there is not only Gaussian noise but also non-Gaussian noise with spikes [16]. The impulsive noise is usually described by the alpha stable distribution [17].

There are many methods for MCLFM parameter estimation, but most of them assume Gaussian noise. In [18], a new parameter estimation method for MCLFM signals based on complex Independent Component Analysis (ICA), second-order time moments, and the Wigner-Hough transform (WHT) was proposed. In [19], a parameter estimation method using the fractional Fourier transform (FRFT) was proposed. Reference [20] proposed a parameter estimation method based on k-resolution FB (k-FB) series expansion combined with dechirp technology. In [21], a method based on nonlinear mode decomposition (NMD) and FRFT was proposed. In [22], FRFT, short-time Fourier transform (STFT), and Hough transform (HT) were used to estimate the parameters of MCLFM signals.

The methods mentioned above cannot accurately estimate the parameters of MCLFM signals in alpha-stable noise. There are very few studies on the parameter estimation of MCLFM signals in alpha-stable noise. In [23], Lv's distribution (LVD), Local Polynomial Periodogram (LPP), and HT were used to estimate parameters, and the influence of alpha-stable noise was suppressed by a limiter. [23] also proposed a MCLFM

This work was supported by the National Natural Science Foundation of China under Grant 62231027 and 62071364, Natural Science Basic Research Program of Shaanxi under Grant 2024JC-JCQN-63, the Key Research and Development Program of Shaanxi under Grant 2023-YBGY-249, the Guangxi Key Research and Development Program under Grant 2022AB46002 and the Innovation Capability Support Program of Shaanxi under Grant 2024RS-CXTD-01. *(Corresponding author: Mingqian Liu.)*

Z. Wen, M. Liu, and X. Yang are with the State Key Laboratory of Integrated Service Networks, Xidian University, Shaanxi, Xi'an 710071, China (e-mail: zx_wen@stu.xidian.edu.cn; mqliu@mail.xidian.edu.cn; yxn2117@126.com).

Y. Chen is with Department of Engineering, University of Durham, Durham, UK DH1 3LE (e-mail: Yunfei.Chen@durham.ac.uk).

N. Zhao is with the School of Information and Communication Engineering, Dalian University of Technology, Dalian 116024, China (e-mail: zhaonan@dlut.edu.cn).

A. Nallanathan is with the School of Electronic Engineering and Computer Science, Queen Mary University of London, London E1 4NS, U.K. (e-mail: a.nallanathan@qmul.ac.uk)

parameter estimation method based on the fractional lower order scaled ambiguity function transform (FLOSAT), but these methods are characterized by high complexity. In [24], a LFM signal parameter estimation method based on fractional low-order covariance (FLOC) fractional spectrum was proposed. While this method can be applied in the presence of alpha-stable noise, it is specifically designed for single-component LFM signal and is not effective for MCLFM signals.

Motivated by the above discussion, we propose a parameter estimation method for MCLFM signals based on the fractional Fourier transform-bald eagle search algorithm (FRFT-BES) and synchroextracting short-time fractional Fourier transform-Hough (SSFT-Hough) with alpha-stable noise in this paper. The main contributions of this paper can be summarized as follows:

- A nonlinear transformation is proposed to suppress alpha-stable noise. It only changes the amplitude and does not affect the phase information of the signal, which has no impact on the parameter estimation of MCLFM signals;
- We improve the Cubic mapping (CM) and combine it with BES, so that BES has better initial population diversity and the performance of its optimal solution is improved;
- FRFT-BES is proposed to estimate the frequency modulation rate of MCLFM signals, which achieves high estimation accuracy;
- We propose a new time-frequency (TF) transfrom method as SSFT to obtain high TF resolution of MCLFM signals;
- SSFT-Hough is proposed to accurately estimate the initial frequency of MCLFM signals.

The remainder of this paper is organized as follows. Section II gives the SCURS model, signal model, and noise model. Section III proposes the parameter estimation method of MCLFM signals. In Section IV, simulation results are presented. Finally, the conclusion is given in Section V.

## II. System Model

### A. SCURS Model

In SCURS, MCLFM and specially designed OFDM signals are combined at the transmitter and then transmitted through the channel with alpha-stable noise $e_{ch}(t)$. Subsequently, they are demodulated separately at the receiving end. The system block diagram of SCURS is shown in Fig. 1 [25], [26].

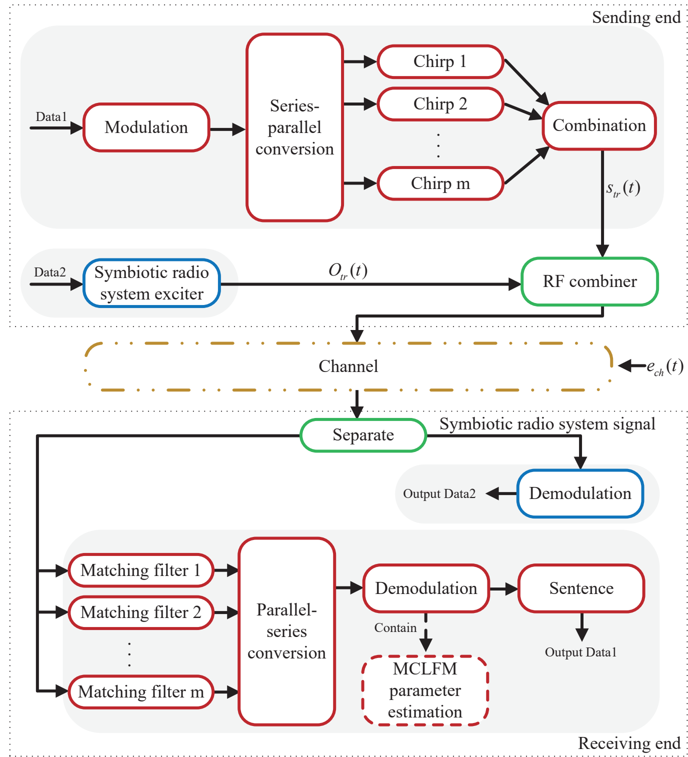


Fig. 1: System block diagram of symbiotic chirp-UWB radio system.

### B. Signal Model

The received signal is represented as

$$SC(t) = s_{tr}(t) + \eta O_{tr}(t) + e_{ch}(t), \tag{1}$$

where $s_{tr}(t)$ is MCLFM signals, $\eta$ denotes the scaling factor, and $O_{tr}(t)$ stands for the OFDM signal. The expression of $s_{tr}(t)$ is given as

$$s_{tr}(t) = \sum_{i=1}^{m} s_i(t), 0 \leq t \leq T, \tag{2}$$

where $s_i(t)$ denotes the $i$th signal of MCLFM signals, $m$ represents the number of LFM signals in SCURS, and $T$ stands for the LFM pulse duration. The expression of $s_i(t)$ is

$$s_i(t) = A_i \exp\left(j\pi\left(2f_i t + k_i t^2\right)\right), \tag{3}$$

where $A_i$, $f_i$, and $k_i$ are amplitude, initial frequency, and frequency modulation rate of $s_i(t)$, respectively. Then we can rewrite (2) by putting (3) into (2) as

$$s_{tr}(t) = \sum_{i=1}^{m} A_i \exp\left(j\pi\left(2f_i t + k_i t^2\right)\right), 0 \leq t \leq T. \tag{4}$$

So we can obtain the separated MCLFM signals as

$$s(t) = s_{tr}(t) + e(t), \tag{5}$$

where $e(t)$ denotes alpha-stable noise.

### C. Noise Model

The alpha stable distribution is usually described by characteristic function (CF) because it does not have a closed form expression of the probability density function (P.D.F.). Its CF is given by [27], [28]

$$\varphi(t) = \exp\{j\sigma t - \rho|t|^{\alpha_e}[1 + j\beta sgn(t) w(t, \alpha_e)]\}, \tag{6}$$

where

$$w(t, \alpha_e) = \begin{cases} \frac{2}{\pi}\log_{10}|t|, \alpha_e = 1, \\ \tan(\frac{\alpha_e \pi}{2}), \alpha_e \neq 1, \end{cases} \tag{7}$$

$$sgn(t) = \begin{cases} 1, t > 0, \\ 0, t = 0, \\ -1, t < 0, \end{cases} \tag{8}$$

where $\sigma$ is the location parameter, $\rho$ stands for the scale coefficient, indicating the dispersion degree of the sample, $\alpha_e$ represents the characteristic exponent with $0 < \alpha_e \leq 2$, which determines the impulsiveness of the alpha stable distribution. Moreover, when $\alpha_e = 2$, the alpha stable distribution becomes the Gaussian distribution; when $\alpha_e = 1$, the alpha stable distribution becomes the Cauchy distribution. $\beta$ denotes the symmetric parameter with $-1 \leq \beta \leq 1$. When $\sigma = 0$, $\beta = 0$, and $\rho = 1$, the alpha stable distribution is called the symmetric alpha stable ($S\alpha S$) distribution. We use the $S\alpha S$ distribution and assume that $1 \leq \alpha_e \leq 2$ in this paper. Due to the absence of the second-order statistics or above, the variance do not exist, and the signal-to-noise ratio (SNR) becomes meaningless. We use the mixed signal-to-noise ratio (MSNR) instead, which is given by [29], [30]

$$MSNR = 10\log_{10}(\frac{\sigma_s^2}{\rho}), \tag{9}$$

where $\sigma_s^2$ denotes the variance of the signal.

## III. Parameter Estimation of MCLFM Signals Based on FRFT-BES and SSFT-Hough

### *A. Frequency Modulation Rate Estimation*

Alpha-stable noise makes the parameter estimation of signals challenging and imprecise. Hence, it is necessary to suppress alpha-stable noise in separated MCLFM signals to make parameter estimation feasible. We propose a nonlinear transformation to suppress alpha-stable noise as

$$z(t) = \frac{0.5^{log_e(|s(t)|)+1}}{e + |s(t)|^{1/e}} s(t). \tag{10}$$

The nonlinear transformation defined above will only affect the amplitude information, not the phase information of the signal. It can eliminate the impact of large pulses on parameter estimation of MCLFM signals.

**Property 1.** *The nonlinear transformation proposed in* (10) *only alters the amplitude information and does not affect the phase information of the separated MCLFM signal.*

*Proof.* See Appendix. □

FRFT is a generalized form of the Fourier transform (FT) and is an effective tool for analyzing the spectrum of LFM signals. In FRFT, if the FT of the signal represents a counterclockwise rotation of the TF plane of the signal by $\pi/2$ around the origin, then the FRFT of the signal is the TF plane of the signal rotated counterclockwise by an angle $\alpha$ around the origin, where $\alpha$ stands for the rotation angle. After the rotation, we can obtain the FRFT domain. The FRFT can be expressed as

$$X_p(u) = \int_{-\infty}^{+\infty} s_{tr}(t) K_p(t,u) dt, \tag{11}$$

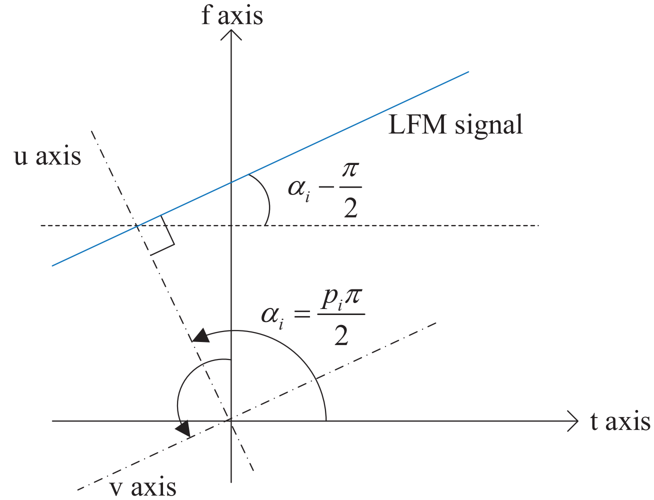


Fig. 2: Geometric relationship between FRFT and TF diagram.

where $p$ represents the order of FRFT with $p = 2\alpha/\pi$ and $p \in [0, 2]$, $K_p(t,u)$ denotes the transformation kernel given by

$$K_p(t,u) = \begin{cases} A_p \exp\left(j\pi(t^2 \cot\alpha + u^2 \cot\alpha - 2ut \csc\alpha)\right), \alpha \neq n\pi, \\ \delta(t-u), \alpha = 2n\pi, \\ \delta(t+u), \alpha = (2n \pm 1)\pi, \end{cases} \tag{12}$$

$\delta(t)$ denotes the unit impulse function and $A_p = \sqrt{1 - j\cot\frac{p\pi}{2}}$. When the u axis is rotated to be perpendicular to the LFM signal, the energy of the LFM signal is optimally gathered, represented as the peak in the three-dimensional space of FRFT. From the peak, we can determine the optimal order and rotation angle through a two-dimensional search (TDS). In the three-dimensional space of FRFT, the TDS is expressed as

$$\{p_i, u_i\} = \arg\max_{p,u} |X_p(u)|, \tag{13}$$

where $p_i$ denotes the optimal order of the $i$th signal and $u_i$ is the value of the u axis corresponding to the $i$th signal at this time. Moreover, $\alpha_i = \frac{p_i \pi}{2}$ is the optimal rotation angle of the $i$th signal. In Fig. 2, we can observe the geometric relationship between FRFT and TF diagram, allowing us to estimate the frequency modulation rate of the $i$th signal in MCLFM signals by $p_i$. However, the $p_i$ obtained by TDS is imprecise. To address this issue, we propose a new method called FRFT-BES. Using FRFT-BES, we can accurately estimate the frequency modulation rate of MCLFM signals.

First, $\{u_i\}$ needs to be obtained for future filtering. The separated MCLFM signals are processed using (10) to obtain $z(t)$. Then, we perform FRFT on $z(t)$ to obtain

$$X_p(u) = \int_{-\infty}^{+\infty} z(t) K_p(t,u) dt. \tag{14}$$

Next, we use TDS to obtain $p_i$ and $u_i$ by (13). According to Fig. 2, we can calculate the normalized frequency modulation rate of the $i$th signal as

$$k_i' = \tan(\alpha_i - \pi/2) = -\cot\alpha_i = -\cot p_i\pi/2. \tag{15}$$

Then we determine the frequency modulation rate of the $i$th signal $k_i$ as

$$k_i = \frac{k_i' f_s}{t_w}, \tag{16}$$

where $f_s$ is the sampling frequency and $t_w$ represents the observation time. To obtain the remaining $p_i$ and $u_i$, we need to filter out the current signal. We perform FRFT on $z(t)$ at order $p_i$ to obtain $X_{p_i}(u)$, then a narrowband band-stop filter $F(u_i)$ is constructed with $u_i$ as the center, and we pass $X_{p_i}(u)$ through the filter as

$$X_{p_i}(u) = X_{p_i}(u)F(u_i). \tag{17}$$

Perform FRFT on $X_{p_i}(u)$ at order $-p_i$ to recover the signal, resulting in $x_r(t)$. Let $z(t) = x_r(t)$ and we can obtain the remaining $p_i$ and $u_i$ by repeating the above procedure. The procedure of the $\{p_i, u_i\}$ estimation of MCLFM signals based on FRFT with alpha-stable noise is summarized in Algorithm 1.

**Algorithm 1** The $\{p_i, u_i\}$ estimation of MCLFM signals based on FRFT

**Require:** $s(t)$ : the separated MCLFM signals; $m$ : the number of LFM signals in SCURS.

**Ensure:** $\{p_i\}$ : the optimal order of MCLFM signals; $\{u_i\}$ : the value of the u axis of MCLFM signals.

1: Take $s(t)$ through the nonlinear transformation by (10) and let i=0;
2: **loop**
3: Let i=i+1;
4: **if** $i > m$ **then**
5: break;
6: **end if**
7: Perform FRFT on $z(t)$ by (14), use TDS to find $p_i$ and $u_i$ by (13);
8: Perform FRFT on $z(t)$ at order $p_i$ by (14) to obtain $X_{p_i}(u)$, construct a narrowband band-stop filter $F(u_i)$ with $u_i$ as the center, pass $X_{p_i}(u)$ through the filter by (17);
9: Perform FRFT on $X_{p_i}(u)$ at order $-p_i$ to obtain $x_r(t)$, let $z(t) = x_r(t)$;
10: **end loop**
11: We can obtain $\{p_i\} = \{p_1, p_2, ..., p_m\}$ and $\{u_i\} = \{u_1, u_2, ..., u_m\}$.

Then, we use the BES to obtain the optimal orders of MCLFM signals, and we improve BES with the improved Cubic mapping (ICM). BES is divided into three stages, which are introduced below [31].

Stage 1 is called the select stage. At this stage, the bald eagle selects a search space and determines an optimal hunting region based on the prey population. The bald eagle then hunts within this optimal hunting region. The mathematical model of this stage is given by

$$P_{i,new} = P_{best} + \alpha_c R_r(P_{mean} - P_i), \tag{18}$$

where $P_{i,new}$ denotes the updated position of the $i$th bald eagle and $P_{best}$ stands for the optimal position for the bald eagle in the current stage. $\alpha_c$ is used to control the position of the bald eagle with (1.5,2), $R_r$ represents the random number with (0,1), $P_{mean}$ is the average position of the bald eagle after its last search, and $P_i$ denotes the position of the $i$th bald eagle.

Stage 2 is called the search stage. During this stage, the bald eagle will search for prey in the optimal hunting region selected during the selection stage, and its flight trajectory is a spiral shape. At this time, the bald eagle constantly adjusts its parameters to move towards the optimal position, and at this stage, the movement of the bald eagle will be more diversified. The mathematical models are expressed in polar coordinates as

$$\theta(i) = a\pi * rand, r(i) = \theta(i) + R * rand, \tag{19}$$

$$xr(i) = r(i)\sin(\theta(i)), yr(i) = r(i)\cos(\theta(i)), \tag{20}$$

$$x(i) = \frac{xr(i)}{max(|xR_r|)}, y(i) = \frac{yr(i)}{max(|yR_r|)}, \tag{21}$$

$$P_{i,new} = P_i + y(i)(P_i - P_{i+1}) + x(i)(P_i - P_{mean}), \tag{22}$$

where $x(i)$ and $y(i)$ denote the position of the bald eagle in coordinate space, and their values are between with (-1,1). $r(i)$ and $\theta(i)$ represent the polar diameter and polar angle of the spiral equation, respectively. $a$ and $R$ are the control parameters for the spiral flight trajectory of the bald eagle with (5,10) and (0.5,2), respectively. $rand$ stands for a random number within (0,1).

Stage 3 is called the swooping stage. In this stage, the bald eagle moves rapidly from the optimal position found in the search stage to the target prey, while other bald eagles in the population also move toward the best point. The mathematical model is in polar coordinates as

$$\theta(i) = a\pi * rand, r(i) = \theta(i), \tag{23}$$

$$xr(i) = r(i)\sinh(\theta(i)), yr(i) = r(i)\cosh(\theta(i)), \tag{24}$$

$$x1(i) = \frac{xr(i)}{max(|xR_r|)}, y1(i) = \frac{yr(i)}{max(|yR_r|)}, \tag{25}$$

$$\begin{aligned} P_{i,new} &= rand * P_{best} + x1(i)(P_i - c_1 P_{mean}) \\ &+ y1(i)(P_i - c_2 P_{best}), \end{aligned} \tag{26}$$

where $c_1$ and $c_2$ are both movement intensity coefficients with (1,2). The fitness value is the maximum absolute value of the FRFT value at the currently searched order $p$ in BES.

However, if BES falls into a local optimal value after population initialization, it will adversely affect the subsequent global search for the optimal values, leading to poor performance. So we improve the Cubic mapping to propose the improved Cubic mapping for population initialization in BES. At the same time, we improve it to achieve a more uniform distribution. First, we use a pseudo-random number to generate the initial value of the ICM sequence by

$$C_1 = rand, \tag{27}$$

where $C_1$ denotes the first number of the ICM sequence. Then use the iterative form of CM to generate the next value as

$$C_{j+1} = \gamma_c C_j(1 - C_j^2), \tag{28}$$

where $\gamma_c$ stands for the control parameter, and $C_j$ represents the $j$th number of the ICM sequence. However, in the distribution of CM, the number distribution close to 0 and 1 is still relatively large, so we use a formula to evaluate all points in CM. The closer the points are to 0 and 1, the higher the probability of being regenerated by $rand$ is. The judgment formula is expressed as

$$|C_{j+1} - 0.5| + 0.05 \geq rand * 0.6. \tag{29}$$

If (29) is satisfied, then $C_{j+1} = rand$. Furthermore, since the search range in FRFT is $p \in [0, 2]$, it is also necessary to determine after each point is obtained whether it meets $rand \geq 0.5$. If so, the value of the current point is increased by 1, so that the sequence values of ICM can be evenly distributed in $[0, 2]$. By repeating the above steps, we can obtain the sequence of ICM. The procedure for obtaining the sequence of ICM is summarized in Algorithm 2.

**Algorithm 2** Acquisition of the ICM sequence

**Require:** $\gamma_c$ : the control parameter; $P_{size}$ : the population of BES.
**Ensure:** $\{C_j\}$ : the sequence of ICM.

Let j=1, initialize the ICM sequence with a pseudo-random number of (0,1) by (27);
**while** $j < P_{size}$ **do**
  Obtain the next value in the ICM sequence by (28);
  **if** $|C_{j+1} - 0.5| + 0.05 \geq rand * 0.6$ **then**
    $C_{j+1} = rand$;
  **end if**
  **if** $rand \geq 0.5$ **then**
    $C_{j+1} = C_{j+1} + 1$;
  **end if**
  $j = j + 1$;
**end while**
We can obtain $\{C_j\} = \{C_1, C_2, ..., C_{P_{size}}\}$.

The distribution of ICM and CM is shown in Fig. 3. From Fig. 3, we can see that ICM has a better uniform distribution than CM. This can lead to a more diverse and uniform initial population distribution of BES, enhance the ability to escape local optimal value, and improve the performance of the algorithm. The procedure of the frequency modulation rate estimation of MCLFM signals based on FRFT-BES with alpha-stable noise is summarized in Algorithm 3.

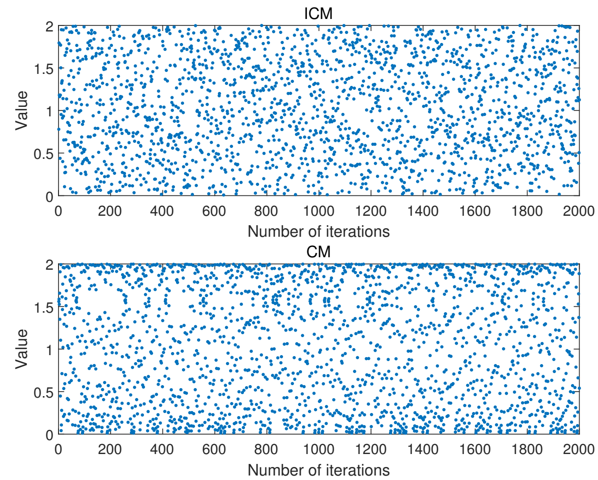


Fig. 3: Distribution of ICM and CM values.

**Algorithm 3** The frequency modulation rate estimation of MCLFM signals based on FRFT-BES

**Require:** $s(t)$ : the separated MCLFM signals; $m$ : the number of LFM signals in SCURS.
**Ensure:** $\{k_i\}$ : the frequency modulation rate of MCLFM signals.

Use Algorithm 1 to get $\{p_i\}$ and $\{u_i\}$;
Take $s(t)$ through the nonlinear transformation by (10) and let i=1;
**while** $i \leq m$ **do**
  Use BES with ICM to obtain the optimal order of $i$th signal $p_i'$, obtain $k_i$ by (15) and (16), let $D = 2$ and $DR = 1$;
  **for** $l = 1$ to $m$ **do**
    $D_1 = |p_i' - p_l|$
    **if** $D_1 < D$ **then**
      $D = D_1$, $DR = l$;
    **end if**
  **end for**
  Perform FRFT on $z(t)$ at order $p_i'$ by (14) to obtain $X_{p_i'}(u)$, construct a narrowband band-stop filter $F(u_{DR})$ with $u_{DR}$ as the center, pass $X_{p_i'}(u)$ through the filter by (17);
  Perform FRFT on $X_{p_i'}(u)$ at order $-p_i'$ to obtain $x_r(t)$, let $z(t) = x_r(t)$;
  Let i=i+1;
**end while**
We can obtain the frequency modulation rate $\{k_i\} = \{k_1, k_2, ..., k_m\}$ and optimal order $\{p_i'\} = \{p_1', p_2', ..., p_m'\}$ of MCLFM signals.

*B. Initial Frequency Estimation*

FT can extract the frequency spectrum of a signal, but it does not provide TF analysis of the signal, so we can not obtain the frequency and time information of the signal simultaneously. To solve this issue, we can use STFT to analyze the signal. STFT can perform TF analysis of the signal, which is given by [32]

$$STFT(t, f) = \int_{-\infty}^{+\infty} [s_{tr}(t)w(u-t)] \exp(-j2\pi f u) du, \tag{30}$$

where $w(t)$ denotes the window function. We use the Gaussian window in this paper as

$$w(t) = \exp(-\frac{10\pi^2 t^2}{3}). \tag{31}$$

However, the STFT is unable to provide high-precision TF analysis, making it difficult to estimate the initial frequency of

MCLFM signals. The short-time fractional Fourier transform (STFRFT) is proposed to enhance the TF resolution. It is a technique that combines STFT and FRFT, which is expressed as

$$STFRFT(t,u)=\int_{-\infty}^{+\infty}s_h(t)w(t-\tau)K_p(t,u)dt. \quad (32)$$

The value on the u axis can be converted to the value on the frequency axis as [33]

$$f_v=\frac{u_v}{\sin\frac{p_v\pi}{2}}, \quad (33)$$

where $u_v$ and $f_v$ represent the values on the u axis and frequency axis, respectively, $p_v$ denotes the order for performing STFRFT. When we take STFRFT of MCLFM signals at the optimal order $p_i'$ of the $i$th signal, in the resulting TF diagram, we can observe that the $i$th signal and other signals of optimal order equal to $p_i'$ are perpendicular to the frequency axis, while the other signals whose optimal order is different from $p_i'$ are not perpendicular to the frequency axis. This principle can be used to estimate the initial frequency of MCLFM signals. To further improve the TF resolution of STFRFT, we propose a novel TF transform method called SSFT based on the concept of synchroextracting transform (SET). SSFT contains STFRFT and its subsequent processing, and it can provide high resolution in TF analysis of signals. This allows for accurate estimation of the initial frequency of MCLFM signals using SSFT. The expression of STFRFT is

$$SR(\tau,u)=\int_{-\infty}^{+\infty}s_h(\tau)Y(\tau-\tau')K_p(\tau,u)d\tau, \quad (34)$$

according to (15) and (16), when $\alpha=2n\pi$ or $\alpha=(2n\pm1)\pi$, $k_i=+\infty$. When $\alpha\neq n\pi$, we can get

$$SR(v,u)=A_p\int_{-\infty}^{+\infty}s_h(v)(Y(v-\tau')H(v,u))^*dv, \quad (35)$$

where

$$H(v,u)=\exp\left(-j\pi(v^2\cot\alpha+u^2\cot\alpha-2uv\csc\alpha)\right), \quad (36)$$

$$A_p=\sqrt{1-j\cot\alpha}, \quad (37)$$

let $g(v)=Y(v-\tau')H(v,u)$, we can obtain

$$\begin{aligned}SR(v,u)&=A_p\int_{-\infty}^{+\infty}s_h(v)g(v)^*dv\\&=\frac{A_p}{2\pi}\int_{-\infty}^{+\infty}S_h(\xi)g(\xi)^*d\xi,\end{aligned} \quad (38)$$

where

$$\begin{aligned}g(\xi)&=\int_{-\infty}^{+\infty}g(v)\exp\left(-j\xi v\right)dv\\&=\int_{-\infty}^{+\infty}Y(v-\tau')H(v,u)\exp\left(-j\xi v\right)dv.\end{aligned} \quad (39)$$

Because the order used for SSFT is the optimal order of the $i$th signal, the signal is perpendicular to the u axis in the spectrum diagram. We can obtain $-\cot\alpha=0$ and $f=u\csc\alpha$ by (15), (16), and the principle of FRFT. Then let $v-\tau'=t'$, we can obtain

$$\begin{aligned}g(\xi)=&\int_{-\infty}^{+\infty}Y(t')H(t',u)\exp\left(-j\xi(\tau'+t')\right)d(\tau'+t')\\&=\exp\left(-j(\xi-\omega)\tau'\right)\int_{-\infty}^{+\infty}Y(t')\exp\left(-j(\xi-\omega)t'\right)dt'\\&=\exp\left(-j(\xi-\omega)\tau'\right)Y_g(\omega-\xi),\end{aligned} \quad (40)$$

where

$$\begin{aligned}H(t',u)=&\exp(-j\pi((\tau'+t')^2\cot\alpha+u^2\cot\alpha\\&-2u(\tau'+t')\csc\alpha)).\end{aligned} \quad (41)$$

Putting (40) into (38), we can get

$$SR(v,\omega)=\frac{1}{2\pi}\int_{-\infty}^{+\infty}S_h(\xi)\exp(j(\xi-\omega)\tau')Y_g(\omega-\xi)d\xi. \quad (42)$$

We take the signal as the pure harmonic signal, which is expressed as

$$s_h(v)=A_s\exp(j\omega_o v), \quad (43)$$

where $A_s$ is the amplitude and $\omega_o$ denotes the instantaneous frequency (IF) of the signal, respectively. Then the FT of the signal is expressed as

$$S_h(\xi)=2\pi A_s\delta(\xi-\omega_o). \quad (44)$$

Using (42), the revised STFRFT can be given by

$$\begin{aligned}SR_e(v,\omega)&=SR(v,\omega)\exp(j\omega\tau')\\&=\frac{1}{2\pi}\int_{-\infty}^{+\infty}2\pi A_s\delta(\xi-\omega_o)Y(\omega-\xi)\exp(j\xi v)d\xi\\&=A_sY(\omega-\omega_o)\exp(j\omega_o v).\end{aligned} \quad (45)$$

Let $v=t$ and take the partial derivative of $SR_e(t,\omega)$ with respect to $t$, we can obtain

$$\begin{aligned}\frac{\partial SR_e(t,\omega)}{\partial t}&=jA_sY(\omega-\omega_o)\exp(j\omega_o t)\omega_o\\&=j\omega_o SR_e(t,\omega),\end{aligned} \quad (46)$$

so

$$\omega_o(t,\omega)=-j\frac{\partial_t SR_e(t,\omega)}{SR_e(t,\omega)}. \quad (47)$$

From (47), it can be seen that when $SR_e(t,\omega)\neq 0$, the IF $\omega_o(t,\omega)$ equals to the STFRFT coefficient for any $(t,\omega)$. Furthermore, there is divergent energy in the TF distribution of the signal, which will result in low TF resolution, so it needs to be removed. Here, we construct a SSFT operator (SSFTO) using a delta function of the form $\delta(\omega-\omega_o(t,\omega))$. SSFTO can be used to eliminate the divergent energy of the signal, allowing for a more concentrated signal energy. By using the SSFTO, we can express the SSFT as

$$SSFT(t,\omega)=SR_e(t,\omega)\delta(\omega-\omega_o(t,\omega)), \quad (48)$$

where

$$\delta(\omega-\omega_o(t,\omega))=\begin{cases}1,\omega=\omega_o(t,\omega),\\0,\omega\neq\omega_o(t,\omega),\end{cases} \quad (49)$$

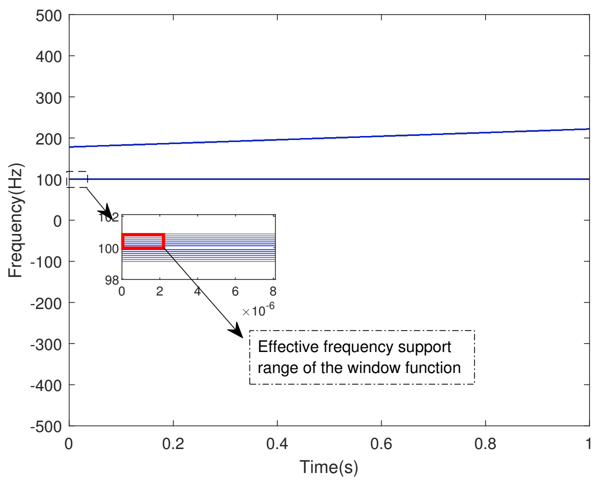


Fig. 4: Effective frequency support range of the window function.

and we can obtain

$$SSFT(t,\omega)=\left\{\begin{array}{c} SR_e(t,\omega), \omega=\omega_o(t,\omega), \\ 0, \omega\neq\omega_o(t,\omega). \end{array}\right. \tag{50}$$

From (50), we know that SSFT can preserve the TF coefficient of the signal at $\omega=\omega_o$ and eliminate the others. Therefore, SSFT can significantly enhance the TF resolution and accuracy of parameter estimation for the signal. For MC signals, SSFT is expressed as [34]

$$SSFT(t,\omega)=SR_e(t,\omega)\delta(\omega-\zeta(t,\omega)), \tag{51}$$

where $\zeta(t,\omega)$ is the sum of MC signals TF resolution with

$$\zeta(t,\omega)=\sum_{i=1}^{m}\zeta_i(t,\omega)=-j\frac{\partial_t SR_e(t,\omega)}{SR_e(t,\omega)}, \tag{52}$$

where $\zeta_i(t,\omega)$ denotes the IF of the $i$th signal. Meanwhile, the IF of MC signals need to satisfy

$$\zeta_{i+1}(t,\omega)-\zeta_i(t,\omega)>2\Delta, \tag{53}$$

where $\Delta$ denotes the effective frequency support range of the window function shown in Fig. 4.

In summary, when we use SSFT to process MCLFM signals, high resolution MCLFM TF diagram will be obtained. However, each time we perform SSFT at order $p_i'$, only the signals with the same order will be perpendicular to the frequency axis, while the rest will not. Therefore, we can only estimate the initial frequency of one signal at a time. Then, HT is used to estimate the initial frequency of MCLFM signals. A straight line in a rectangular coordinate system can be expressed as

$$\omega=Ct+Z, \tag{54}$$

where $\omega$ and $t$ represent the vertical axis and horizontal axis of the TF domain, respectively. $C$ and $Z$ represent the slope and intercept of the straight line, respectively. By using HT, the line detection problem can be transformed into a peak detection problem. The peak detection of the point can then provide the intercept and slope of the straight line. So, HT can transform a straight line in the rectangular coordinate system into a point in the polar coordinate system, and the transformation is given by

$$\gamma=t\cos\theta+\omega\sin\theta, \tag{55}$$

where $\gamma$ is the distance between the central point and the straight line in the polar coordinate system, and $\theta$ denotes the angle between the normal line and the horizontal axis. When we perform SSFT on MCLFM signals at order $p_i'$, the TF distribution of the $i$th signal will be perpendicular to the $\omega$ axis. We can use HT to detect all TF distributions of MCLFM signals and identify all peaks. Then, we can locate the $\theta_i$ closest to $-\pi/2$ and determine its corresponding $\gamma_i$, where $\theta_i$ and $\gamma_i$ denote the $\gamma$ and $\theta$ of the $i$th signal, respectively. If more than one $\gamma_i$ is found, we can choose one arbitrarily. Next, the intercept of $s_i(t)$ can be given as

$$u_{v_i}=\frac{f_s}{2}-f_s(|\gamma_i|+l_{ws}\Delta/l_{TF}), \tag{56}$$

where $l_{ws}$ stands for the compensating number and $l_{TF}$ denotes the height of the TF diagram. We can obtain the initial frequency of the $i$th signal by (33). Similar to the frequency modulation rate estimation, a two-dimensional filter is constructed to filter the SSFT spectrum and isolate the TF distribution of $s_i(t)$. Subsequently, the inverse SSFT transformation is performed to restore the signal. Finally, the initial frequency can be estimated by repeating the above steps. The procedure of initial frequency estimation of MCLFM signals based on SSFT-Hough with alpha-stable noise is summarized in Algorithm 4.

**Algorithm 4** The estimation of initial frequency for MCLFM signals based on SSFT-Hough

**Require:** $s(t)$ : the separated MCLFM signals; $m$ : the number of LFM signals in SCURS; $\{p_i'\}$ : the optimal order of MCLFM signals.
**Ensure:** $\{f_i\}$ : the initial frequency of MCLFM signals.
1: Take $s(t)$ through the nonlinear transformation by (10) and let i=1;
2: **while** $i\leq m$ **do**
3: Perform SSFT on $x(t)$ at order $p_i'$;
4: Use HT for MCLFM signals to get all peaks, find $\theta_i$ closest to $-\pi/2$ and get its corresponding $\gamma_i$;
5: Obtain the the intercept of $s_i(t)$ by (56);
6: Estimate the initial frequency $f_i$ of $s_i(t)$ by (33);
7: Construct a two-dimensional filter, filter the SSFT spectrum to isolate the TF distribution of $s_i(t)$. Then perform the inverse SSFT transformation to restore the signal $x_r(t)$, let $z(t)=x_r(t)$;
8: Let $i=i+1$;
9: **end while**
10: We can obtain $\{f_i\}=\{f_1,f_2,...,f_m\}$.

## IV. Simulation Results and Analysis

To verify the proposed parameter estimation method, we conduct MATLAB simulation. In MCLFM signals, the number of signals is $m=2$, the frequency modulation rates are

$k_1 = 100Hz/s$ and $k_2 = 50Hz/s$, the initial frequencies are $f_1 = 200Hz$ and $f_2 = 100Hz$, the sampling frequency is $f_s = 1000Hz$, the observation time is $t_w = 1s$, the control parameter is $\gamma_c = 2.595$, the population size of FRFT-BES is $P_{size} = 30$, and the population size of FRFT-particle swarm optimization (FRFT-PSO) is the same as that of FRFT-BES, the maximum number of iterations for FRFT-BES and FRFT-PSO is 45, and the noise distribution is the $S\alpha S$ distribution. In parameter estimation, the performance is measured by the normalized root mean square error (NRMSE), which is given as follows

$$NRMSE = \sqrt{\sum_{q=1}^{N} \left( Z - \hat{Z}(q) \right)^2 / (N \cdot Z^2)}, \tag{57}$$

where $N$ is the number of Monte Carlo simulation experiments, $Z$ is the actual value of the parameter, $\hat{Z}(q)$ is the $q$th estimated value of the parameter. We set $N$ to 300 in this paper. Moreover, we also carried out the success rate experiment for frequency modulation rate estimation comparison. The success rate is given by

$$S_{Rate} = \frac{N_s}{2N}, \tag{58}$$

where $N_s$ denotes the number of successful estimation. A successful estimation is achieved when the modulus of the difference between the estimated frequency modulation rate and the true frequency modulation rate is less than or equal to 0.5.

In Fig. 5, when $MSNR = -5dB$ and $\alpha_e = 1$, we use different methods for TF analysis of MCLFM signals. From Fig. 5a and Fig. 5b, it can be observed that, when MSNR is low, if we use STFT and STFRFT to do TF analysis of MCLFM signals, the TF characteristics of each signal will be overwhelmed by alpha-stable noise. This leads to poor TF resolution, making it difficult to estimate the initial frequency. From Fig. 5c and Fig. 5d, it is seen that the proposed method not only effectively suppresses alpha-stable noise but also preserves the TF characteristics of each signal. Additionally, it has good TF resolution, laying a solid foundation for the initial frequency estimation. So the proposed method can effectively estimate the initial frequency of MCLFM signals with alpha-stable noise and offers superior TF resolution compared to STFT and STFRFT.

For performance comparison, we use the FRFT and PSO based method for parameter estimation of single-component LFM signal as mentioned in [36]. This is within the framework of the proposed method without ICM as FRFT-PSO, which is capable of estimating the parameters of MCLFM signals. In Fig. 6 and Fig. 7, we compare the performance of the proposed method with FRFT-PSO and FRFT under the same experimental conditions when $\alpha_e = 1$ in frequency modulation rate estimation. From Fig. 6, as the MSNR increases, the NRMSE of the frequency modulation rate estimated by FRFT remains around $7.4 \times 10^{-3}$. However, the NRMSE of FRFT-PSO is higher than that of FRFT only when $MSNR = -10dB$. In all other cases, it improves with increasing MSNR and always outperforms FRFT. In comparison, the NRMSE of the proposed method is always better than FRFT and FRFT-PSO, reaching approximately $2.1 \times 10^{-3}$ at high MSNR. Moreover, we compare the success rate of the proposed method with FRFT and FRFT-PSO in Fig. 7. From Fig. 7, it can be observed that as the MSNR increases, the success rate of FRFT stays at 50% all the time, while the success rate of FRFT-PSO consistently outperforms it and can eventually reach 92%. In addition, the success rate of the proposed method consistently outperforms the other two methods and reaches 99% at high MSNR. Therefore, the proposed method has good performance and outperforms FRFT and FRFT-PSO in frequency modulation rate estimation.

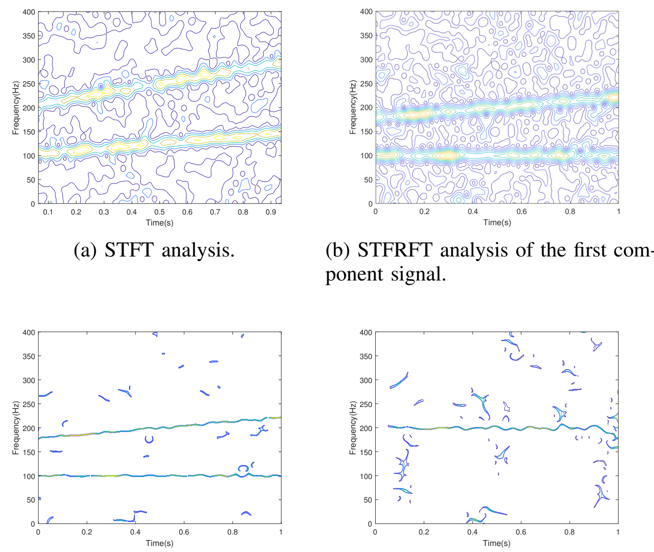

(a) STFT analysis. (b) STFRFT analysis of the first component signal.

(c) SSFT analysis of the first component signal. (d) SSFT analysis of the second component signal.

Fig. 5: TF analysis of MCLFM signals with STFT, STFRFT, and SSFT.

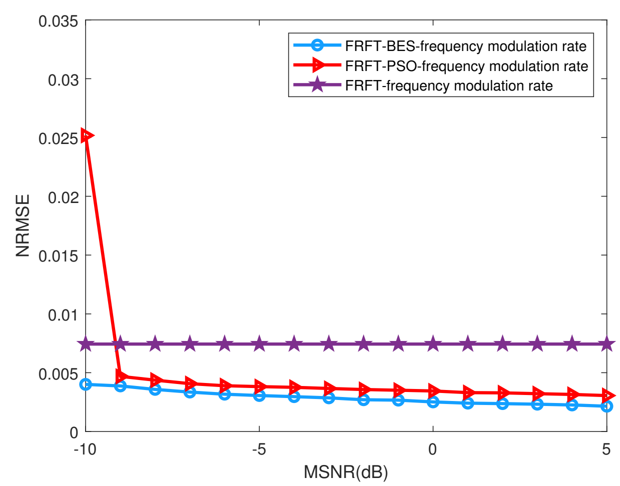


Fig. 6: Estimation performance comparison of frequency modulation rate with different methods.

In Fig. 8, we compare the convergence process of FRFT-BES and FRFT-PSO under the same experimental conditions when $\alpha_e = 1$ and $MSNR = -10dB$ in frequency modulation

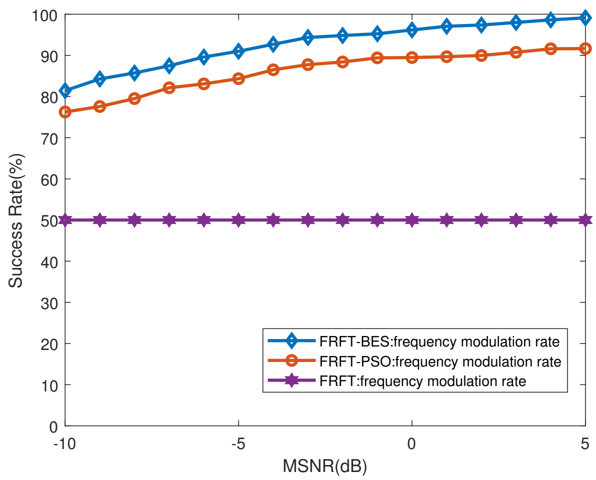


Fig. 7: Success rate comparison of frequency modulation rate estimation with different methods.

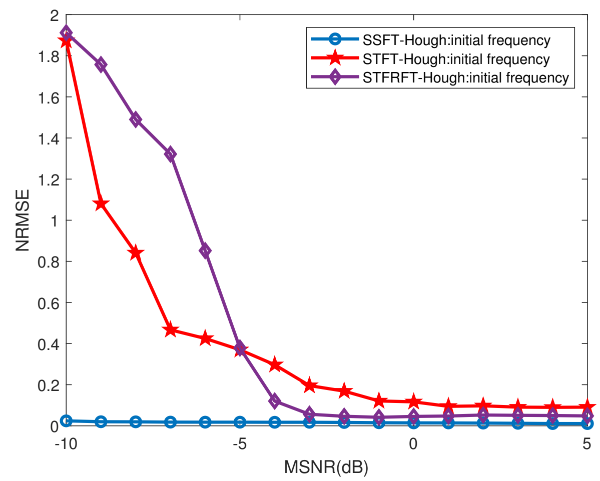


Fig. 9: Estimation performance comparison of initial frequency with SSFT-Hough, STFT-Hough, and STFRFT-Hough.

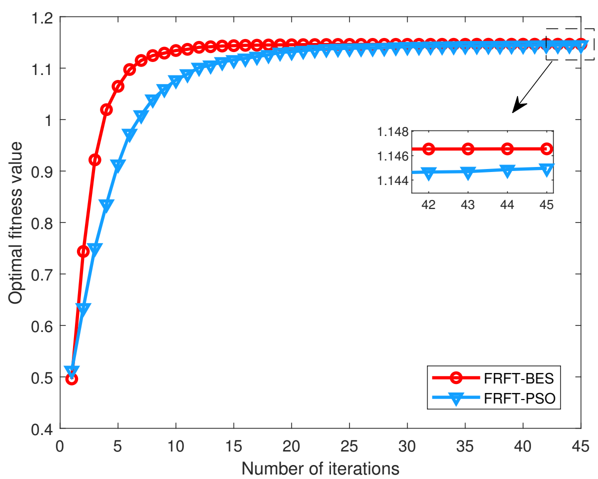


Fig. 8: Convergence process comparison of frequency modulation rate estimation with different methods.

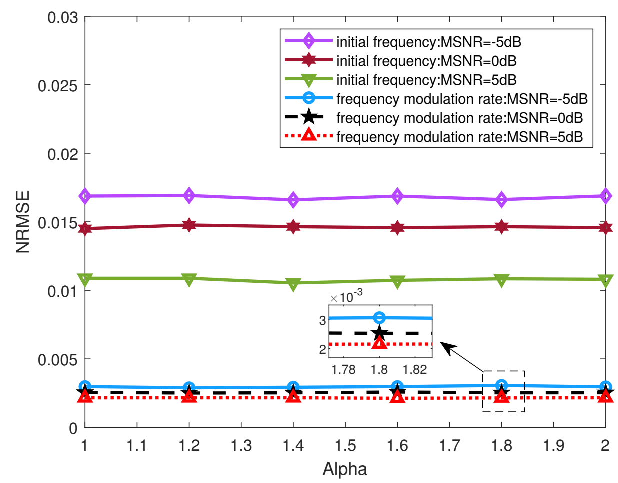


Fig. 10: Estimation performance of frequency modulation rate and initial frequency under different characteristic exponents.

rate estimation. From Fig. 8, we can find that FRFT-BES converges more rapidly than FRFT-PSO with the increase of iterations. Besides, the optimal fitness value of FRFT-BES in the final search result is greater than that of FRFT-PSO, confirming that FRFT-BES has better performance than FRFT-PSO in frequency modulation rate estimation. Therefore, the proposed method has better search performance than FRFT-PSO.

In Fig. 9, we compare the initial frequency estimation performance of STFT-Hough, STFRFT-Hough, and the proposed method under different MSNR in the same experimental condition when $\alpha_e = 1$. From Fig. 9, with the increase of MSNR, the NRMSE of STFT-Hough eventually decreases to around $9 \times 10^{-2}$, and the NRMSE of STFRFT-Hough is better than STFT-Hough only when $MSNR \geq -4dB$, which is going to end up around $5 \times 10^{-2}$. Meanwhile, the NRMSE of the initial frequency estimated by the proposed method is consistently less than $2.5 \times 10^{-2}$, which is significantly lower than that of STFT-Hough and STFRFT-Hough. The optimal NRMSE of the proposed method in initial frequency estimation is approximately $1 \times 10^{-2}$. In summary, the proposed method performs well and outperforms STFT-Hough and STFRFT-Hough.

In Fig. 10, we analyze the estimation performance of the frequency modulation rate and initial frequency for different characteristic exponents and different MSNR. From Fig. 10, when $MSNR \geq -5dB$, the estimation performance of the frequency modulation rate and initial frequency remains stable under different characteristic exponents. So the proposed method is not affected by the characteristic exponent, demonstrating its robustness to the characteristic exponent at low MSNR in the $S\alpha S$ distribution.

In Fig. 11 and Fig. 12, we compare the parameter estimation performance of different methods under different characteristic exponents when $MSNR = 0dB$. From Fig. 11, we can see that across different characteristic exponents, the frequency

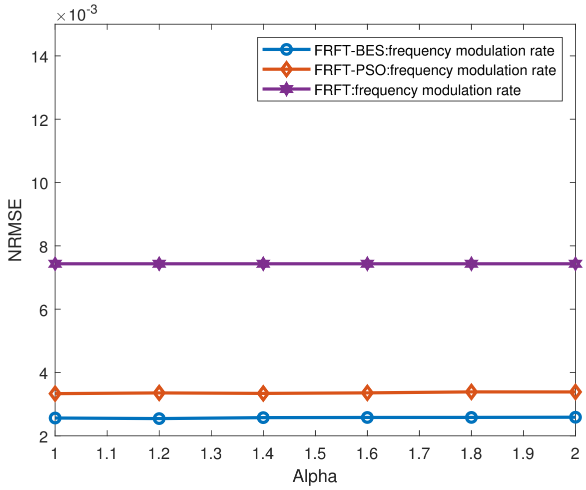


Fig. 11: Frequency modulation rate estimation performance comparison of different methods with different characteristic exponents.

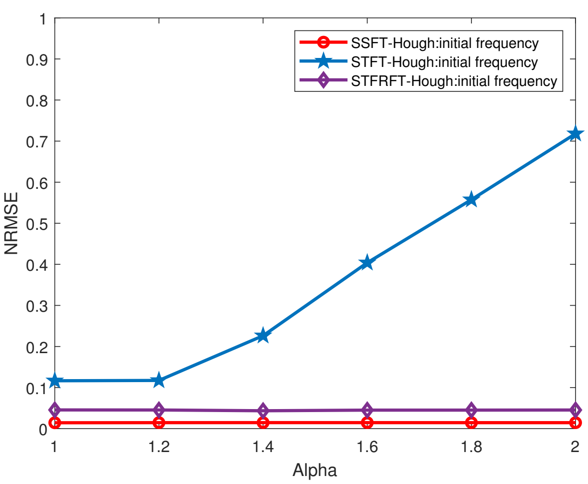


Fig. 12: Initial frequency estimation performance comparison of different methods under different characteristic exponents.

modulation rate estimation performance of all three methods remains consistent respectively, demonstrating the stability of the three methods. Moreover, the NRMSE of the proposed method remains stable at around $2.5 \times 10^{-3}$, which is an improvement over the $7.4 \times 10^{-3}$ of FRFT and the $3.3 \times 10^{-3}$ of FRFT-PSO. From Fig. 12, we can observe that as the characteristic exponent increases, the NRMSE of STFT-Hough also increases. In contrast, the NRMSE of STFRFT-Hough and the proposed method remains constant, indicating that STFT-Hough is unstable while the other two methods are stable. In addition, the NRMSE of the proposed method is stable at approximately $1.45 \times 10^{-2}$, which is better than the $4.35 \times 10^{-2}$ of STFRFT-Hough and STFT-Hough with a minimum value of $1.1 \times 10^{-1}$. So we know that the proposed method has better performance, stability, and feasibility compared to the other two methods in the $S\alpha S$ distribution.

## V. Conclusion

This paper proposes a new parameter estimation method for MCLFM signals with alpha-stable noise in SCURS, which can assist in the demodulation of SCURS. In order to suppress alpha-stable noise without affecting the parameter estimation, we develop a nonlinear transformation to reduce the amplitude of MCLFM signals with alpha-stable noise. Next, we use FRFT to obtain the parameters required for filtering and improve CM to obtain ICM. Then, we use ICM to enhance BES to estimate the frequency modulation rate of MCLFM signals. In addition, we propose a high resolution TF transform method called SSFT and combine it with HT to propose SSFT-Hough to estimate the initial frequency. Moreover, simulation results demonstrate that the proposed parameter estimation method is effective and feasible at low MSNR, and it has good performance. At the same time, the performance of the proposed method has been significantly improved compared to existing methods.

## Appendix
## Proof of Property 1

The expression of the nonlinear transformation can be expressed as

$$\begin{aligned} z(t) &= \frac{0.5^{log_e(|s(t)|)+1}}{e+|s(t)|^{1/e}} s(t) \\ &= \frac{0.5^{log_e(|\sum\limits_{i=1}^{m} s_i(t)+e(t)|)+1}\left(\sum\limits_{i=1}^{m} s_i(t)+e(t)\right)}{e+|\sum\limits_{i=1}^{m} s_i(t)+e(t)|^{1/e}}. \end{aligned} \tag{59}$$

In this paper, we study three kinds of nonlinear transformations, and their discussion is given as follows.

1) When MSNR is large, which is $|\sum\limits_{i=1}^{m} s_i(t)| \gg |e(t)|$, then $s(t) \approx \sum\limits_{i=1}^{m} s_i(t) = \sum\limits_{i=1}^{m} A_i \exp\left(j\pi\left(2f_i t + k_i t^2\right)\right)$, and we can get

$$\begin{aligned} z(t) &= \frac{0.5^{log_e(|s(t)|)+1}}{e+|s(t)|^{1/e}} s(t) \\ &\approx \frac{0.5^{log_e(|\sum\limits_{i=1}^{m} s_i(t)|)+1}}{e+|\sum\limits_{i=1}^{m} s_i(t)|^{1/e}} s(t) \\ &= \frac{0.5^{log_e(|\sum\limits_{i=1}^{m} A_i \exp(j\pi(2f_i t+k_i t^2))|)+1}}{e+|\sum\limits_{i=1}^{m} A_i \exp\left(j\pi\left(2f_i t+k_i t^2\right)\right)|^{1/e}} s(t) \\ &= J(t)s(t), \end{aligned} \tag{60}$$

where $J(t)$ denotes a real number and it is defined as

$$J(t) = \frac{0.5^{log_e(|\sum\limits_{i=1}^{m} A_i \exp(j\pi(2f_i t+k_i t^2))|)+1}}{e+|\sum\limits_{i=1}^{m} A_i \exp\left(j\pi\left(2f_i t+k_i t^2\right)\right)|^{1/e}}. \tag{61}$$

2) When MSNR is small, which is $|\sum_{i=1}^{m} s_i(t)| \ll |e(t)|$, then $s(t) \approx e(t)$, and we can obtain

$$\begin{aligned} z(t) &= \frac{0.5^{log_e(|s(t)|)+1}}{e+|s(t)|^{1/e}} s(t) \\ &\approx \frac{0.5^{log_e(|e(t)|)+1}}{e+|e(t)|^{1/e}} s(t) \\ &= J_1(t)s(t), \end{aligned} \tag{62}$$

where $J_1(t)$ represents a real number and it is expressed as

$$J_1(t) = \frac{0.5^{log_e(|e(t)|)+1}}{e+|e(t)|^{1/e}}. \tag{63}$$

3) When MSNR approaches to zero, which is $|\sum_{i=1}^{m} s_i(t)| \approx |e(t)|$, and we can obtain

$$\begin{aligned} z(t) &= \frac{0.5^{log_e(|s(t)|)+1}}{e+|s(t)|^{1/e}} s(t) \\ &= \frac{0.5^{log_e(|\sum_{i=1}^{m} A_i \exp\left(j\pi\left(2f_i t + k_i t^2\right)\right)+e(t)|)+1}}{e+|\sum_{i=1}^{m} A_i \exp\left(j\pi\left(2f_i t + k_i t^2\right)\right)+e(t)|^{1/e}} s(t) \\ &= J_2(t)s(t), \end{aligned} \tag{64}$$

where $J_2(t)$ stands for a real number and is given by

$$J_2(t) = \frac{0.5^{log_e(|\sum_{i=1}^{m} A_i \exp\left(j\pi\left(2f_i t + k_i t^2\right)\right)+e(t)|)+1}}{e+|\sum_{i=1}^{m} A_i \exp\left(j\pi\left(2f_i t + k_i t^2\right)\right)+e(t)|^{1/e}}. \tag{65}$$

From (60), (62), and (64), we can conclude that the nonlinear transformation changes the amplitude without changing the phase information of the separated MCLFM signals.

## REFERENCES


[1] Z. Lv, H. Fan, Z. Chen, J. Qiu, M. Ren and Z. Zhang, "Mitigate the LFM-PRFI in SAR Data: Joint Down-Range and Cross-Range Filtering," *IEEE Trans. Geosci. Remote Sens.*, vol. 61, no. 5205918, pp. 1-18, April 2023.

[2] J. H. Park and S. C. Park, "Complex Range Resolution Model of Point Scatterers in LFM Chirp Pulse Radar," *IEEE Trans. Instrum. Meas.*, vol. 71, no. 4506112, pp. 1-12, Sept. 2022.

[3] M. Liu, Z. Zhang, Y. Chen, J. Ge and N. Zhao, "Adversarial Attack and Defense on Deep Learning for Air Transportation Communication Jamming," *IEEE Trans. Intell. Transp. Syst.*, vol. 25, no. 1, pp. 973-986, Jan. 2024.

[4] J. Zhang, M. Liu, Y. Chen, N. Zhao and A. Nallanathan, "Automatic Identification of Space-Time Block Coding for MIMO-OFDM Systems in the Presence of Impulsive Interference," *IEEE Trans. Commun.*, early access, March 28, 2024, doi: 10.1109/TCOMM.2024.3382326.

[5] Z. Wei, N. Fu, S. Jiang, X. Li and L. Qiao, "Parameter Measurement of LFM Signal With FRI Sampling and Nuclear Norm Denoising," *IEEE Trans. Instrum. Meas.*, vol. 71, no. 2002417, pp. 1-17, March 2022.

[6] G. Wei, M. Li and H. Zhao, "The General Evaluation Model for Radio-Frequency Blocking Effects of Frequency Equipment in Complex Electromagnetic Environment," *IEEE Trans. Antennas Propag.*, vol. 71, no. 9, pp. 7418-7425, Sept. 2023.

[7] H. -Z. Zhao, G. -H. Wei and X. -D. Pan, "Evaluation Method of Noise Electromagnetic Radiation Interference Effect," *IEEE Trans. Electromagn. Compat.*, vol. 65, no. 1, pp. 69-78, Feb. 2023.

[8] R. Long, Y. -C. Liang, H. Guo, G. Yang and R. Zhang, "Symbiotic Radio: A New Communication Paradigm for Passive Internet of Things," *IEEE Internet Things J.*, vol. 7, no. 2, pp. 1350-1363, Feb. 2020.

[9] F. Jameel, S. Zeb, W. U. Khan, S. A. Hassan, Z. Chang and J. Liu, "NOMA-Enabled Backscatter Communications: Toward Battery-Free IoT Networks," *IEEE Internet Things Mag.*, vol. 3, no. 4, pp. 95-101, Dec. 2020.

[10] N. Jin, G. Yang, Y. -C. Liang, S. Fu and X. Chen, "Joint Beamforming and Backscatter Communication Design for Symbiotic Radio Networks," *IEEE Internet Things J.*, vol. 10, no. 22, pp. 19441-19453, Nov. 2023.

[11] G. Yang, Z. Luo, N. Jin, Y. -C. Liang, Y. Xu and G. Wang, "Non-Coherent Parallel Detection of Ambient Backscatter Communications With Multiple Tags," *IEEE Trans. Veh. Technol.*, vol. 72, no. 4, pp. 5344-5349, April 2023.

[12] Y. -C. Liang, Q. Zhang, E. G. Larsson and G. Y. Li, "Symbiotic Radio: Cognitive Backscattering Communications for Future Wireless Networks," *IEEE Trans. Cognit. Commun. Networking*, vol. 6, no. 4, pp. 1242-1255, Dec. 2020.

[13] Y. -C. Liang, Q. Zhang, J. Wang, R. Long, H. Zhou and G. Yang, "Backscatter Communication Assisted by Reconfigurable Intelligent Surfaces," in *Proc. IEEE*, Sept. 2022, pp. 1339-1357.

[14] F. Jameel, R. Duan, Z. Chang, A. Liljemark, T. Ristaniemi and R. Jantti, "Applications of Backscatter Communications for Healthcare Networks," *IEEE Netw.*, vol. 33, no. 6, pp. 50-57, Nov.-Dec. 2019.

[15] M. Luan, B. Wang, Z. Chang, T. Hämäläinen and F. Hu, "Robust Beamforming Design for RIS-Aided Integrated Sensing and Communication System," *IEEE Trans. Intell. Transp. Syst.*, vol. 24, no. 6, pp. 6227-6243, June 2023.

[16] J. Zhang, N. Zhao, M. Liu, Y. Chen, F. Gong, Q. Yang and F. R. Yu, "Transmit Antenna Number Identification for MIMO Cognitive Radio Systems in the Presence of Alpha-Stable Noise," *IEEE Trans. Veh. Technol.*, vol. 71, no. 3, pp. 2798-2808, March 2022.

[17] Y. Zhang and Y. Zhang, "An Adaptive Parameter Estimation Algorithm of Radar Linear Frequency Modulation Signal Based on Nonlinear Transform Under Different Alpha Stable Distribution Noise Environments," *IEEE J. Miniaturization Air Space Syst.*, vol. 4, no. 4, pp. 389-399, Dec. 2023.

[18] G. Qiang, L. Ya-jun, W. Chang-hong and C. He-yang, "Novel Detection Method for Multi-component LFM Signals," in *Proc. First Int. Conf. Pervasive Comput., Signal Process. Appl.*, Sept. 2010, pp. 759-762.

[19] M. Liu and G. Liu, "Detection of Multicomponent LFM Signal Based on Fractional Fourier Transform," *Electron. Sci. Technol.*, vol. 27, no. 10, pp. 133-135, Oct. 2014.

[20] Q. He, Q. Zhang, Y. Luo and B. Liang, "Multi-component LFM Signal Separation Based on k-FB Series Expansion," *J. Air Force Eng. Univ.*, vol. 18, no. 4, pp. 60-65, Aug. 2017.

[21] T. Yang, J. Shao, Y. Chen and Y. Zhao, "Parameter estimation of multi component LFM signals based on nonlinear mode decomposition and FrFT," in *Proc. Tenth Int. Conf. Adv. Comput. Intell. (ICACI)*, March 2018, pp. 204-209.

[22] F. Xu, Q. Bao, Z. Chen, S. Pan and C. Lin, "Parameter Estimation of Multi-Component LFM Signals Based on STFT+Hough Transform and Fractional Fourier Transform," in *Proc. 2nd IEEE Adv. Inf. Manage., Communicates, Electron. Autom. Control Conf. (IMCEC)*, May 2018, pp. 839-842.

[23] P. Duan, "Parameter Estimation of Linear Frequency Modulated Signals in Complicated Noise Environment," M.S. thesis, Dept. School Electron. Eng., Xidian Univ., Xi'an, China, 2014.

[24] G. -D. Gu, Y. -S. Zhang and B. Tian, "Estimation of LFM Signal's Time Parameters under the alpha-Stable Distribution Noise," in *Proc. IEEE Circuits Syst. Int. Conf. Test. Diagn.*, April 2009, pp. 1-4.

[25] F. Wang, X. Chen, A. Men, L. Zhang and S. Wu, "Carrier frequency offset estimation for FM and symbiotic FM radio data system hybrid signal," *China Commun.*, vol. 17, no. 1, pp. 129-139, Jan. 2020.

[26] P. Zhang, H. Liu and J. Hu, "A Novel Multiple-Access Scheme for Chirp UWB," in *Proc. IEEE Wireless Commun. Networking Conf.*, March 2007, pp. 1631-1635.

[27] J. Wang, E. E. Kuruoglu and T. Zhou, "Alpha-Stable Channel Capacity," *IEEE Commun. Lett.*, vol. 15, no. 10, pp. 1107-1109, Oct. 2011.

[28] S. Luan, Y. Gao, J. Zhou and Z. Zhang, "Automatic Modulation Classification Based on Cauchy-Score Constellation and Lightweight Network Under Impulsive Noise," *IEEE Wireless Commun. Lett.*, vol. 10, no. 11, pp. 2509-2513, Nov. 2021.

[29] S. Ma, C. Zhao and Y. Wang, "Fractional Low Order Cyclostationary Spectrum Sensing Based on Eigenvalue Matrix in Alpha-Stable Distribution Noise," in *Proc. First Int. Conf. Pervasive Comput., Signal Process. Appl.*, Sept. 2010, pp. 500-503.

[30] J. Li, D. -Z. Feng and W. X. Zheng, "A Robust Decision Directed Algorithm for Blind Equalization Under $\alpha$-Stable Noise," *IEEE Trans. Signal Process.*, vol. 69, pp. 4949-4960, July 2021.

[31] H. A. Alsattar, A. A. Zaidan and B. B. Zaidan, “Novel meta-heuristic bald eagle search optimisation algorithm,” *Artif. Intell. Rev.*, vol. 53, no. 3, pp. 2237-2264, July 2019.

[32] P. Pietrzak and M. Wolkiewicz, “Stator Phase Current STFT analysis for the PMSM Stator Winding Fault Diagnosis,” in *Proc. Int. Symp. Power Electron., Electr. Drives, Autom. Motion (SPEEDAM)*, June 2022, pp. 808-813.

[33] J. Li, R. Jin, J. Geng, Y. Fan and W. Mao, “Detection and Estimation of Multi-component LFM Signals Based on Gauss Short-Time Fractional Fourier Transform,” *J. Electron. & Inf. Technol.*, vol. 29, no. 3, pp. 570-573, March 2007.

[34] G. Yu, M. Yu and C. Xu, “Synchroextracting Transform,” *IEEE Trans. Ind. Electron.*, vol. 64, no. 10, pp. 8042-8054, Oct. 2017.

[35] M. Liu, Y. Han, Y. Chen, H. Song, Z. Yang and F. Gong, “Modulation Parameter Estimation of LFM Interference for Direct Sequence Spread Spectrum Communication System in Alpha-Stable Noise,” *IEEE Syst. J.*, vol. 15, no. 1, pp. 881-892, March 2021.

[36] Q. Meng, G. Shao and B. Wang, “Identification and Parameter Estimation of Underwater LFM Signals Under $\alpha$-Stable Distribution Noise,” in *Proc. 8th Int. Conf. Electron. Inf. Emerg. Commun. (ICEIEC)*, June 2018, pp. 190-193.